Volume 1 | Number 1 | Jan 2013 | Pages 1–100

Metallomics

Integrated biometal science
www.rsc.org/metallomics

ROYAL SOCIETY OF CHEMISTRY

ROYAL SOCIETY OF CHEMISTRY

www.rsc.org/metallomics

Journal Name

ARTICLE

Antiangiogenic ruthenium(II) benzimidazole complexes, structure-based activation of distinct signaling pathways

Haoqiang Lai,[‡] Zhennan Zhao,[‡] Linlin Li, Wenjie Zheng, Tianfeng Chen*

Antiangiogenic therapy is considered to be a promising strategy for the treatment of cancers. VEGF and its receptors are important angiogenic factors involved in tumor growth. In the present study, the new ruthenium(II) complexes containing 2, 6-bis (benzimidazolyl) pyridine have been identified as potent antiangiogenic agents *in vitro* and *in vivo*, through activation of distinct antiangiogenic signaling pathways. Specifically, [Ru(bbp)(*p*-mpip)Cl]ClO$_4$ (complex **2**, bbp = 2, 6-bis (benzimidazolyl) pyridine; *p*-mpip = 2-(4-methylphenyl)imidazo[4,5-f]-1,10-phenanthroline) exhibited the highest antiangiogenic activity, as evidenced by significant suppression of neovessel formation in chick chorioallantoic membrane and blockage of the angiogenesis in a matrigel plugs assay, which are significantly higher than those of the most accepted anti-metastasis ruthenium-based drug NAMI-A. Generally, this kind of complexes induced G0/G1cell cycle by inhibiting the formation of Cyclin D1/CDK4 complex and CDK2 activation, through up regulation of the expression levels of p15^{INK4B}, p21^{Cip1} and p27^{Kip1}. Moreover, the complexes also triggered intracellular DNA damage, and thus activated the phosphorylation of ATM, ATR, CHK1, Histone and p53. The suppression of Akt and ERK1/2 pathways reinforced the cell cycle perturbation effects of the complexes. Interestingly, complex **2** displayed strong inhibition on the activation of VEGF and VEGFR-2 phosphorylation, which blocked the transmission of the mitogenic signal through Akt and ERK1/2 pathways, and thus enhanced cell cycle arrest. In contrast, we found that the most accepted anti-metastasis ruthenium based drug NAMI-A exerted lower antiangiogenic *via* activation of DNA damage-mediated pathway, but showed no effects on VEGF and VEGFR-2 phosphorylation. Taken together, this study clearly demonstrate the distinct antiangiogenic mechanisms of metal complexes, and this kind of complexes can be further developed as anti-vascularized drugs as alternative agent of NAMI-A in treatment of cancers.

Introduction

Angiogenesis plays an essential role in carcinogenesis, cancer progression and metastasis[1-3]. Tumor angiogenesis is important for the delivery of essential nutrients and oxygen to the tumour microenvironment, which promotes the transformation of small, dormant cancers into invasive and metastatic forms[4-5]. Substantial evidence has supported that new blood formation is extremely critical for stolid tumour invasion, to growth beyond a critical size or metastatic mass beyond 2 to 3 mm[6-7]. Especially for highly-vascularized tumors, even though after surgery and radiotherapy, patients may still face dying as a result of metastasis and cancer recurrence. In recent decades, many studies have supported that blocking angiogenesis was an efficient strategy to inhibit tumor growth and metastasis[8-9]. Therefore, identification and development of new effective antiangiogenic agents continues to be a topic of intense research.

Recent studies have reported the *in vitro* and *in vivo* anti-angiogenic effects of metallodrugs, including ruthenium (Ru), cobal and gold complexes[10-15]. Numerous Ru complexes have been synthesized and demonstrated anticancer potency owing to their attracting cellular functions, including targeting cellular proteins[16], induction of apoptosis[17-18] and antimetastatic effects[19]. Recent reports showed that Ru complexes could inhibit cancer angiogenesis *in vitro* and *in vivo*[20]. Especially, NAMI-A, as the most accepted antimetastatic drug, was able to restrain cancer metastasis by suppressing metallo-proteinases[21]. Studies have showed that series of Ru(II) complexes exhibit higher antiangiogenic activity properties than NAMI-A.[20,22-24] However, the underlying molecular mechanisms accounting for the antiangiogenic activity of Ru complex remain elusive.

Metallomics Accepted Manuscript

Our previous studies showed that the Ru(II) complexes containing bis-benzimidazole derivatives exhibited higher *in vitro* anticancer activities than NAMI-A by targeting mitochondria and induction of caspase-dependent apoptosis[25]. Ru(II) complexes containing benzimidazole (a wildly used pharmacophore[26]) exhibited outstanding potency in anticancer, anti-Alzheimer, anion-sensing and photophysical studies.[27-32] However, little information about the antiangiogenic activities of Ru(II) benzimidazole complexes is available. Therefore, we investigated the antiangiogenic activities and explored the underlying molecular mechanisms of a series of Ru(II) benzimidazole complexes.(**Fig. 1A**)

Results and discussion

Synthesis and characterization of Ru(II) complexes

Firstly, the synthetic Ru complexes were synthesized and characterized by ESI-MS, ^1H NMR and elemental analysis to confirm their chemical structures. (see the Experimental section for further details and **Fig. S1–S2** in ESI for the mass spectrometry and ^1H NMR spectra of Ru complexes **2** and **3**). We also examined the stability of Ru complexes (30 µM) in PBS buffer by UV-Vis spectroscopy. As shown in **Fig. S3**, no obvious change in the UV-Vis absorption spectra of Ru complexes during 72 h incubation was observed. The lipophilicity of the Ru complexes was examined by determining the distribution coefficients (log P) using the "shake-flask" method. As shown in **Fig. 1B**, the structure changes of R group affected the lipophilicity and cellular uptake of the Ru complexes. For instance, the introduction of electron-donating group (-CH$_3$) into the ligand 2-phenyl-imidazo[4,5-f]1,10-phenanthroline in complex **2** increased the lipophilicity, thus contribute to higher cellular uptake in HUVECs. In contrast, the introduction of electron-withdrawing group (-NO$_2$) into the ligand reduced these properties. Endothelial cell proliferation is essential in the multi-step process of angiogenesis. We next examined whether the Ru(II) complexes could modulate the proliferation of endothelial cells (1.5×10^4 cells/mL) within 72 h by using MTT assay. As illustrated by **Fig. S4A**, the change of substituent groups of the complexes significantly affected inhibitory activities of Ru(II) complexes against HUVECs. In contrast, NAMI-A was less effective than the synthetic Ru(II) complexes. For instance, complex **1**, **2** and **3** at 20 and 40 µg/mL exhibited different inhibitory effects on the proliferation of HUVECs, but no significant inhibition was observed in cells exposed to 20-80 µg/mL NAMI-A. Only slight inhibition was observed at 160 µg/mL NAMI-A. Furthermore, we also examined the cytotoxicity of these complexes at a cell density of 5×10^4 cells/mL for 24 h. We found that Ru(II) complexes (40 µg/mL) and NAMI-A (160 µg/mL) slightly suppressed proliferation of HUVECs in such condition. The above results indicate that Ru complexes could inhibit angiogenesis in HUVECs at non-toxic or sub-toxic dose.
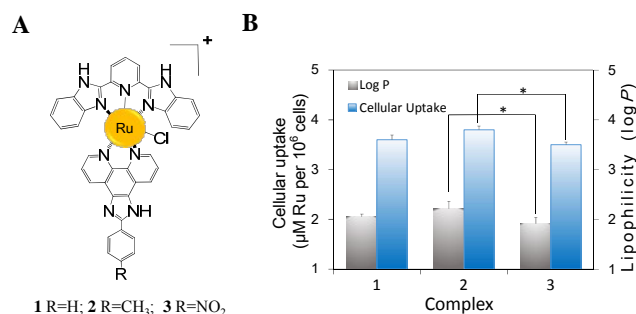

1 R=H; **2** R=CH$_3$; **3** R=NO$_2$

Fig. 1. (A) Structure of the synthetic Ru(II) complexes in this study. (B) The relationship between cellular uptake and lipophilicity of complexes. Significant difference between different groups is indicated at *P*< 0.05 (*).

Ru(II) complexes suppress VEGF-induced migration, invasion and capillary structure formation.

As cell migration and invasion are necessary for angiogenesis and critical for tumour growth and metastasis, we employed wound-healing migration assay and Transwell assay to detect the antiangiogenic action of Ru (II) complexes in this study. The results showed that, Ru (II) complexes at sub-toxic concentrations (40 µg/mL) strongly suppressed VEGF-induced migration and invasion of HUVECs (**Fig. 2A**-**D**). Similar suppression effects were also observed on HUVECs exposed to NAMI-A. However, the inhibition action was inferior to the synthetic Ru(II) complexes, even at the concentration raised up to 160 µg/mL. These results reveal that the new class of complexes strongly inhibited the VEGF-induced migratory and invasive process of endothelial cells.

To further determine the effects of Ru(II) complex on angiogenesis, two-dimensional Matrigel assay was employed to investigate how these novel agents regulates the capillary tubule formation of HUVECs. After exposed to VEGF, elongated and robust tube-like structures were formed, while obviously disruption of capillary tube formation was observed in cells exposed to the complexes **1**, **2** and **3** (**Fig. 2E-F**). On the contrary, the formation of capillary-like structures was less inhibited by NAMI-A. In all, the above results demonstrated that Ru (II) complexes performed more effective suppression on VEGF-induced angiogenesis than NAMI-A.

Ru(II) complexes restrain angiogenesis *ex ovo* and *in vivo*.

Because the higher potency of the synthetic complex **2** against angiogenesis, further studies were carried out to examine the *ex ovo* and *in vivo* anti-angiogenic activities. As illustrated in **Fig. 3A**, complex **2** (40 µg/mL) exhibited higher anti-angiogenic effect than NAMI-A (160 µg/mL) *ex ovo* in CAM model. Although the density of the vascular plexus was increased with the presence of VEGF, complex **2** still dramatically suppressed
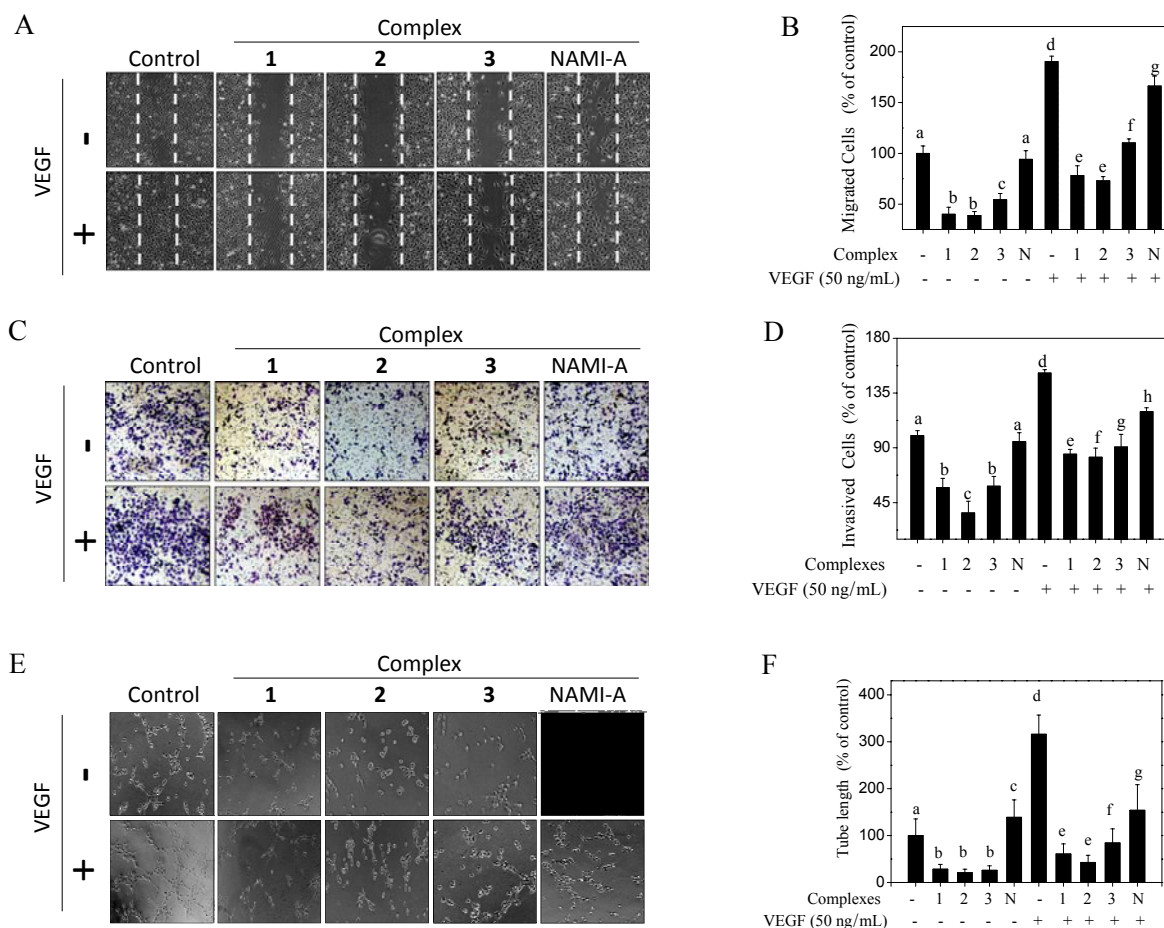
Fig.2. Ru complexes inhibit VEGF-induced migration of HUVECs. (A) Ru complexes inhibit VEGF-induced HUVECs migration. (B) Quantitative analysis of the migrated cells by manual counting. (C) Assessment of invasion inhibition of HUVECs after exposure to Ru complexes. (D) Cells migrated to the bottom of the membrane were quantified by manual counting. (E) Ru complexes inhibit VEGF-induce tube formation of HUVECs. HUVECs were seeded in 48-well plates pre-coated with matrigel and treated with Ru complexes for 8 h. (F) Formation of cell tubular structures was quantified by manual counting under an inverted microscope. All the cells were treated with or without 50 ng/mL VEGF and 40 μg/mL Ru(II) complexes or 160 μg/mL NAMI-A, and compared with control group with 0.5% DMSO solution in culture medium. All images shown here are representative of three independent experiments with similar results. All data here are expressed as means ± SD of triplicates. N is abbreviation for NAMI-A. Bars with different characters (a-h) are statistically different at $P<0.05$ level.

the VEGF-enhanced new capillary formation from the pre-existing vascular network (**Fig. 3B**). It should be noted that this effect is seen at the 40 μg/mL dose, which is sub-toxic concentrations to inhibit the growth of HUVECs. Matrigel plug assay was also used to evaluate the effects of complex **2** on the VEGF-induced angiogenesis *in vivo*. In this study, Matrigel containing VEGF (50 ng/mL), with or without 20 and 40 μg/mL complex **2** was injected (s.c.) into the ventral area of the 6 weeks old male C57/BL/6 mice (six mice for each group). Fourteen days later, the plugs were removed. As shown in **Fig. 3C**, the plugs containing Matrigel alone did not induce or induce less blood vessel formation, while those containing VEGF alone displayed dark red colour. The vessels were abundant in red blood cells, indicating the formation of angiogenesis-promoted vasculature inside the Matrigel. In contrast, the red colour in the VEGF complex **2** (20 μg/mL) group was dramatically inhibited. Specifically, when the

concentration of complex **2** raised up to 40 μg/mL, the vasculature formation was totally suppressed as evidenced by pale in colour, which suggest that treatment of complex **2** antagonizes the VEGF-induced sprouting in a dose-dependent manner (**Fig. 3C**). In concomitant, the antiangiogenetic effect of complex **2** was further confirmed by H&E staining. More and thicker erythrocyte-containing vessels were also detected in VEGF group by H&E staining, however, which was effectively inhibited by treatment of complex **2**. Further study by determination of hemoglobin content confirmed that complex **2** effectively inhibited the formation vasculature and presence of red blood cells in a dose-dependent manner (**Fig. 3D**), which suggest that the synthetic Ru complex may attenuate cancer angiogenesis *in vivo*.[33] As one of the most important pro-angiogenic molecules, the expression of VEGF was also significantly inhibited by complex **2**. Taken together, these
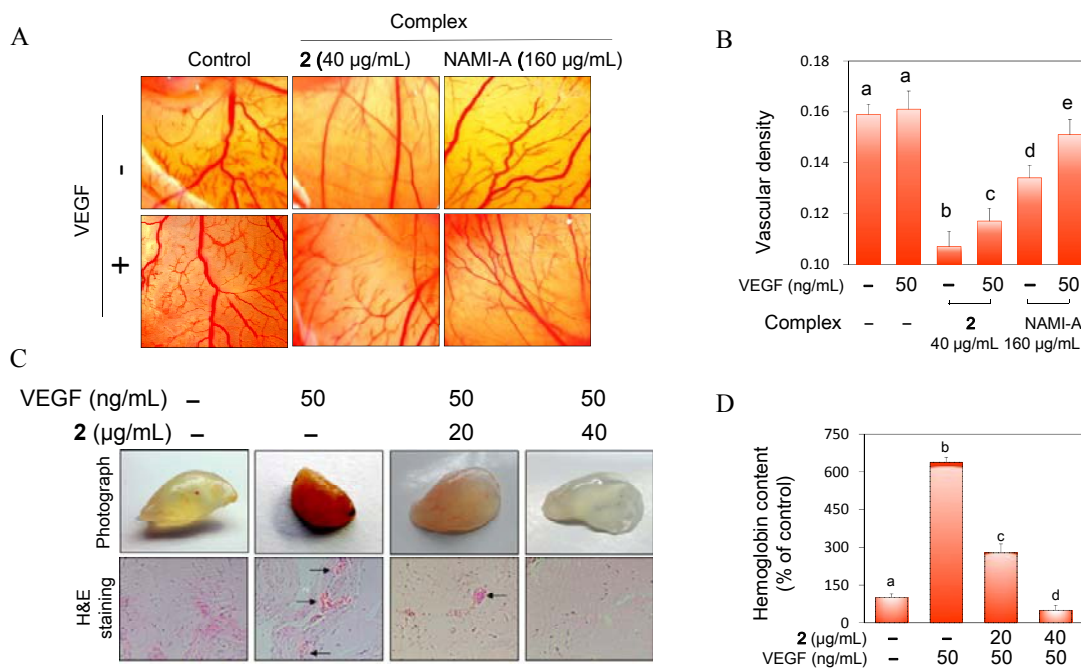
Fig.3. Complex 2 inhibits new blood formation in CAM *ex ovo* and angiogenesis *in vivo*. (A) Representative images of angiogenesis inhibition of complex in CAM assay. Complex **2** (40 µg/mL) or NAMI-A (160 µg/mL) with or without 50 ng/mL VEGF were treated on CAM surface 7 or 8-day-old chick embryos. (B) Quantitation of vascular density base on the CAM images. (C) Complex **2** inhibits angiogenesis in Matrigel plug assay. Six-week-old C57/BL/6 mice were injected with 500 µL Matrigel containing VEGF and complex **2** (20, 40µg/mL). After 7 d, the matrigel plugs were harvested and representative Matrigel plugs were photographed. The Matrigel plugs were fixed with formalin, sectioned, stained with H&E. The arrows indicate the formation of blood vessel. (D) Quantitation of active vasculature inside the Matrigel by measurement of hemoglobin content. Hemoglobin was quantified and presented compared with the control. All results are compared with control group with 0.5% DMSO solution added in the experiments. Bars with different characters (a-d) are statistically different at *P*<0.05 level.

results clearly demonstrate the synthetic Ru(II) complexes as potent antiangiogenic agents.

Induction of G0/G1 arrest and apoptosis through triggering DNA damage.

Following, flow cytometric analysis was carried out to examine the effects of the synthetic Ru complexes on HUVEC cell cycle distribution. As depicted in **Fig. 4A**, Ru complexes induced G0/G1 arrest and apoptosis in HUVECs in a dose-dependent manner. For instance, after 72-h incubation with 20, 40, and 80 µg/mL of complex **2**, the cells in G0/G1 phase were remarkably enhanced by 6.8, 13.3, and 21.5%, respectively, which was accompanied by a concomitant decrease in cell populations at S and G2/M phases. On the other hand, we found that the Ru(II) complexes **1** remarkably influenced the cell cycle through increased the sub-G1 population, but complex **3** induced cell apoptosis in a moderate manner (**Fig. 4B**). In contrast, NAMI-A only slightly affect the cell cycle, which implies the significant difference in the apoptotic-inducing capacity between these metal complexes. Taken together, these results suggest that Ru(II) complexes possess more potent antiproliferative activities toward HUVECs than NAMI-A *via* different action mechanisms.
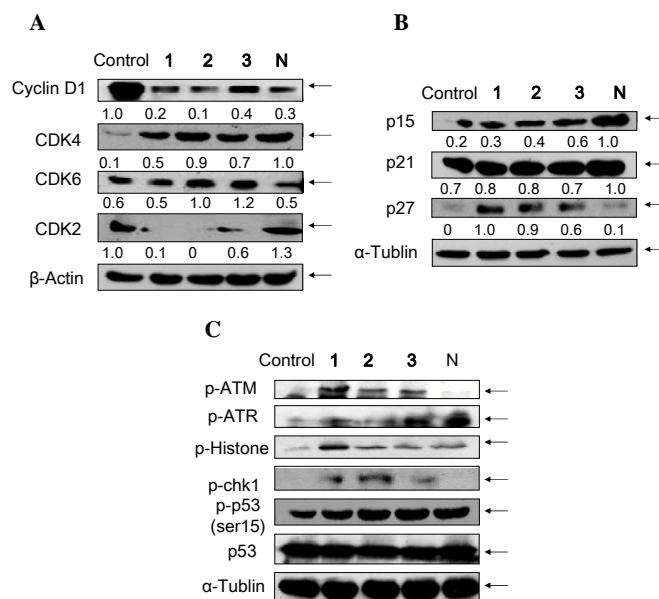
Cell cycle is tightly controlled by many regulators, such as cyclins, cyclin-dependent kinase (CDKs), CDK inhibitors, and growth suppressor genes. In this study, we have found that the synthetic Ru(II) complexes induced G0/G1 arrest in HUVECs.

Therefore, experiments were conducted to evaluate the proteins levels of cell cycle regulators involved in this effect by Western blotting. The results showed that the expression level of cyclin D1 was strongly inhibited by the treatment of the complexes. Meanwhile, the expression level of CDK4 increased obviously, which may be due to the accumulation of HUVECs at this phase. Interestingly, different expression profiles of CDK6 and CDK2 were found in cells exposed to NAMI-A and the synthetic Ru(II) complexes. For instance, NAMI-A exhibited no effect on the expression of CDK6, but increased the expression of CDK2. In contrast, the complexes **2** and **3** up-regulated the expression level of CDK6, but strongly suppressed the expression of CDK2 (**Fig.5A**). Furthermore, the effects of Ru(II) complexes on the expression level of several CDK inhibitors, including $p15^{INK4b}$, $p21^{waf1/Cip1}$ and $p27^{Kip1}$, were examined in this study. As revealed in **Fig.5B**, different changes were observed in HUVECs exposed to NAMI-A and Ru(II) complexes. Specifically, treatment of NAMI-A resulted in higher up-regulation of $p15^{INK4b}$ and $p21^{waf1/Cip1}$, and lower increase in $p27^{Kip1}$ expression by comparing with the synthetic complexes. These results demonstrate the distinct regulation mechanisms of NAMI-A and the synthetic complexes on the cell cycle progression. Cell cycle arrest and apoptosis are two of the most common cellular response to DNA damage.
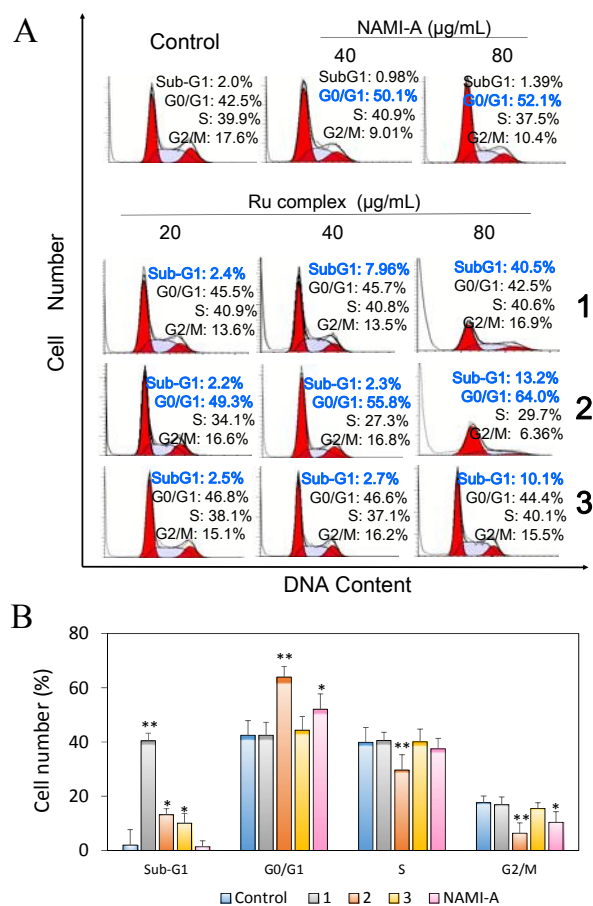
Fig. 4. Different effects on cell cycle induced by Ru complexes as examined by propidium iodide (PI)-flow cytometric analysis. (A) Cells (1.5×10^4 cells/mL) were treated with different concentrations of complexes or 0.5% DMSO in control group for 72 h. (B) Quantitative cell-cycle distribution data for HUVECs after treatment with complexes (80 μg/mL).

Fig. 5. DNA damage mediate-cell cycle arrest in G0/G1 phase of HUVECs induced by Ru complexes. (A) Expression level of cyclin D1, CDK4, CDK6 and CDK2. (B) Expression level of p15[INK4B], p21[Cip1], p27[Kip1]. (C) Ru complexes induced activation of ATM, ATR, Histone, CHK1 and p53. Cells (1×10^5 cells/mL) were treated with 80 μg/mL Ru(II) complexes or NAMI-A for 72 h. The results of Western blot were representatives of three independent experiments with similar results.

With the occurrence of DNA damage, ATM (ataxi a telangiec tasia mutated) and ATR (ataxia telangiectasia) will be activated, which in turn phosphorylates the downstream checkpoint kinases CHK1 and CHK2, as well as tumor suppressor gene p53. Moreover, ATM/ATR, CHK2/CHK1 and p53 pathways cooperate to regulate cell-cycle progression and apoptosis in mammalian cells. Therefore, we also conducted experiments to investigate the effects of Ru(II) complexes on the expression levels of these proteins. As shown in **Fig. 5C**, Ru(II) complexes displayed different effects on the phosphorylation of ATM, ATR, CHK1, p53 and Histone. Among them, complex **1** appeared to be more potent in inducing the phosphorylation of ATM and Histone, while NAMI-A stimulated higher levels of ATR phosphorylation instead of ATM, as accompanied by activation p53 and Histone. Moreover, the synthetic Ru(II) complexes significantly induced the phosphorylation of CHK1, which was not observed in cells exposed to NAMI-A. Taken together, these results clear demonstrate the difference in the regulation mechanisms of DNA damage-triggered signaling among the Ru(II) complexes.

Regulation of VEGFR-2-mediated signalling pathways by Ru(II) complexes.

VEGF has been considered as a pivotal chemotactic agent in initiating angiogenesis, and VEGF-VEGFR signaling pathway is now identified as key factor in developmental angiogensesis of many stolid tumours.[34] In the present study, we have showed that Ru(II) complexes could significantly suppress VEGF-induced angiogenesis *in vitro* and *in vivo*. Therefore, we further investigated whether these complexes could suppress VEGF secretion and the tyrosine phosphorylation of VEGFR-2 (the active form of VEGFR-2) in HUVECs. As shown in **Fig. 6A**, different response in VEGF-VEGFR signaling pathway was observed in cells exposed to the Ru(II) complexes. For instance, complex **2** almost thoroughly eliminated the expression of total and phosphorylated VEGFR-2, while **1** merely targeted VEGF without affecting VEGFR-2. However, NAMI-A showed no effects on VEGF-VEGFR-2 signaling, suggesting that other pathways may be involved in antiangiogenic action of this complex.

Activation of VEGFR-2 may consequently result in activation of several downstream pathways, such as Akt and ERK1/2 signal pathways. Studies have showed that blocking Akt[35] and ERK1/2[36] pathways could achieve efficient angiogenesis inhibition. Consequently, we detected whether the Akt and ERK1/2 signal pathways were involved in angiogenesis inhibition induced by Ru(II) complexes. As

Metallomics Accepted Manuscript
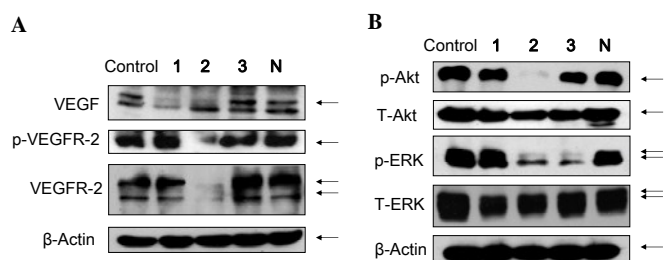
Fig. 6. Ru complexes restrained VEGF, VEGFR-2 tyrosine kinase activity and VEGFR-2 signaling pathway. (A) Complexes inhibited the secretion of VEGF, proteins expression level of phosphorylation of VEGFR-2 and total VEGFR-2. (B) Complexes inhibited VEGFR-2 downstream signaling molecules, including p-ERK/ERK and p-AKT/AKT. Cells (1×10^5 cells/mL) were treated with 80 µg/mL Ru(II) complexes or NAMI-A for 72 h. All results of Western blot were representatives of three independent experiments with similar results.
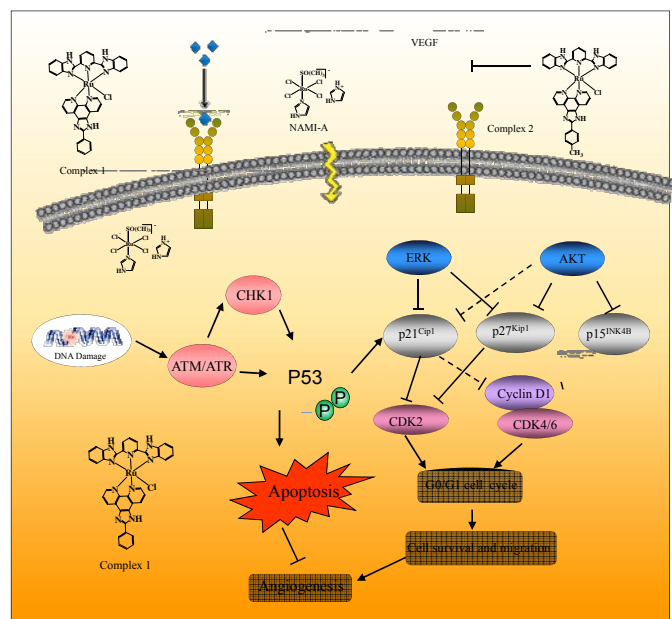
Fig. 7. Antiangiogenic signaling pathways triggered by Ru complexes in HUVECs.

shown in **Fig. 6B**, complex **2** strongly induced the dephosphorylation of Akt and ERK1/2, without affecting the total expression level on Akt and ERK1/2. Furthermore, complex **3** significantly decreased the expression level of phosphorylated ERK1/2, and slightly suppressed the phosphorylation of Akt. However, differently, NAMI-A exhibited no significant effects on the phosphorylation of ERK1/2 and Akt.

Reactive oxygen species (ROS), as endogenous modulators of VEGFR-2, have been identified to play an important role in angiogenesis[37]. Therefore, in this study, we also detected the change in ROS level by measuring the DCF fluorescence intensity. The results showed that, Ru(II) complexes significantly decreased the intracellular ROS generation in a dose-dependent manner, while the ROS generation was less inhibited by NAMI-A, which may account for the difference cellular molecular mechanism between

NAMI-A and these Ru(II) complexes (**Fig. S5A**). Furthermore, time courses of ROS generation inducted by complexes (40 µg/mL) were also displayed in **Fig. S5B**. Treatment of cells with Ru(II) complexes obviously decreased the intracellular ROS level within 2 h, while treatment of NAMI-A didn't show significant effect on ROS level. Therefore, DPPH and ABTS free radical scavenging assays were applied to examine the total antioxidant activities of the Ru complexes. After addition of the complexes, a rapid onset of scavenge DPPH and ABTS free radicals by synthetic Ru complex was observed (**Fig. S5C-D**). These different antioxidant activities may contribute to the distinct regulation effects of Ru(II) complexes on the downstream signalling pathways.

Conclusions

In summary, we have synthesized a new series of mixed-ligand Ru(II) complexes containing benzimidazolyl, and investigated their antiangiogenic activities and explored the underlying molecular mechanisms in the present study (**Fig. 7**). The results showed that these synthetic Ru(II) complexes significantly inhibited the proliferation, VEGF-induced migration, invasion and tube formation of HUVECs. Ru complex **2** exhibited the highest antiangiogenic activity, as evidenced by significant suppression of neovessel formation in chick chorioallantoic membrane and blockage of the angiogenesis in a matrigel plugs assay, which are significantly higher than those of the most accepted anti-metastasis ruthenium-based drug NAMI-A. The studies on the underlying molecular mechanisms revealed that these synthetic Ru(II) complexes strongly inhibited the activation of VEGF and VEGFR-2 phosphorylation, which blocked the transmission of the mitogenic signal through Akt and ERK1/2 pathways, and thus enhanced cell cycle arrest. In contrast, Ru complexes **1**, **3** and NAMI-A exerted lower antiangiogenic *via* activation of DNA damage-mediated pathway, but showed no effects on VEGF and VEGFR-2 phosphorylation. They induced the phosphorylation of ATM/ATR and Histone, accompanied by activation p53. Moreover, the synthetic Ru(II) complexes significantly induced the phosphorylation of CHK1, which was not observed in cells exposed to NAMI-A. The crosstalk among angiogenic signal axis and p53, AKT and MAPKs pathways may contribute to the intrinsic antiangiogenic effects of Ru(II) complexes. Taken together, this study clearly demonstrate the distinct antiangiogenic mechanisms of Ru complexes, and this kind of complexes can be further developed as anti-vascularized drugs as alternative agent of NAMI-A in treatment of cancers.

Experimental

General

3-[4, 5-dimethyl-thiazol-2-yl]-2, 5-diphenyltetrazolium bromide (MTT), bicinchoninic acid (BCA) kit for protein determination were purchased from Sigma-Aldrich. Endothelial cell growth medium (ECGM), fetal bovine serum (FBS) and the

antibiotic mixture (penicillin-streptomycin) were purchased from Invitrogen (Carlsbad, CA). All antibodies used in this study were purchased from Cell Signaling Technology (Beverly, MA). Recombinant VEGF-A165 was obtained from BD Bioscience Company (NJ, USA). Ru complexes used in experiment were dissolved in DMSO solution.

Syntheses of the ligands

The ligands *p*-mpip, *p*-npip[38] and bbp[25] were synthesized according to reported procedures.

Synthesis of [Ru(bbp)(pip)Cl]ClO$_4$(1)

Complex **1** was prepared according to our previous study.[39]

Synthesis of [Ru(bbp)(*p*-mpip)Cl]ClO$_4$ (2)

Complex **2** was prepared according to the same procedure as described by our previously study[25] with Ru(III)(bbp)Cl$_3$ (0.1296 g, 0.25mmol) and *p*-mpip (0.0776 g, 0.25 mmol). Yield: 40.1%. Found (%): C, 54.7; H, 3.3; N, 14.8. Calc. for C$_{39}$H$_{27}$Cl$_2$N$_9$O$_4$ Ru (%): C, 54.6; H, 3.2; N, 14.7%. ESI-MS: m/z 755.5 (M -ClO$_4$)$^+$, 377.7 (M-ClO$_4$)$^{2+}$. UV-Vis (λ (nm), ε/10^4(M^{-1}cm^{-1})): 288 (4.75); 512 (0.60). ^{1}H NMR (DMSO-d^6, δ ppm): 11.2 (d, 1H), 9.4 (s, 1H), 8.82 (s, 1H), 8.49 (s, 1H), 8.32 (m, 2H), 8.20 (d, 2H), 7.52-7.42 (m, 4H), 7.25 (t, 2H), 7.17(t, 2H), 6.81 (t, 2H), 6.84 (t, 2H), 6.61 (t, 2H), 5.95 (d, 2H) and 1.97 (d,3H).

Synthesis of [Ru(bbp)(*p*-npip) Cl]ClO$_4$ (3)

3 was prepared according to the same procedure as described in [Ru(bbp)(*p*-mpip)Cl]ClO$_4$ with the ligand *p*-npip (0.085 g, 0.25 mmol) in place of pip. Yield: 36.0%. Found (%): C, 51.5; H, 2.5; N, 15.9. Calc. for C$_{38}$H$_{24}$Cl$_2$N$_{10}$O$_6$Ru (%): C, 51.4; H, 2.7; N, 15.8%. ESI-MS: m/z 781.5 (M-ClO$_4$)$^+$, 391.1 (M-ClO$_4$)$^{2+}$. UV-Vis (λ (nm), ε/10^4(M^{-1}cm^{-1})): 288 (3.46); 332 (3.42) 439 (1.44). ^{1}H NMR (DMSO-d^6, δ ppm): 11.28 (d, 2H), 9.38 (d, 1H), 9.12 (s, 1H), 8.75 (d, 2H), 8.51 (s, 1H), 8.38 (d, 2H), 8.30 (m, 2H), 7.93 (t, 1H), 7.70 (t, 1H), 7.49-7.42 (m, 4H), 7.15 (t, 2H), 6.83 (t, 1H) 6.61 (t, 1H) and 6.95 (d, 2H).

Synthesis of [H2im][trans-Ru(III)Cl$_4$(dmso-S)(Him)] (NAMI-A)

[trans-Ru(III)Cl$_4$(Me$_2$SO)$_2$][(Me$_2$SO)$_2$H] complex prepared as previous described[25]. The final product was characterized by ESI mass spectrometry: m/z = 389.7 [Ru(III)Cl$_4$(DMSO)(Him)]$^-$, m/z = 244 [Ru(III)Cl$_4$]$^-$.

Stability of Ru complexes in PBS buffer

The stability of the Ru complexes in PBS buffer was examined by UV-Vis spectrometry. The spectrum of complex (30μM) was recorded after incubation at 37 °C at different periods of time.[39]

Distribution coefficients

The distribution coefficients of Ru complexes (100 μM) were determined by the "shake-flask" method. The mixed solution was shaken 100 times, equilibrated for 4.5 h, and then subjected to ICP-AES analysis.[40]

Cellular uptake of Ru

ICP-AES method was performed to determine the cellular uptake efficiency of Ru complexes (40 μM) in HUVECs after 6-h treatment [39].

Cell culture, determination of cell viability and cell cycle progression

HUVECs were cultivated in endothelial cell growth medium (ECGM):M199 medium (Life Technologies, Invitrogen) supplemented with 15% fetal bovine serum (FBS, Gibco) at 37°C in a humidified (5% CO$_2$, 95% air) atmosphere. The cells were seeded for 24 h, and then treated with Ru complexes (dissolved in DMSO at stock solution of 10 mg/mL) for indicated times. The cell viability of HUVECs was determined by the MTT assay which was carried out as described previously.[41] The effects of the Ru complexes on the cell cycle distribution was examined by PI-staining flow cytometric analysis on Beckman Coulter Flow Cytometer Cytomics FC 500 [42]. The apoptotic cells with hypodiploid DNA content were detected by quantifying the subG1 peak by CXP software. And then, cell cycle distribution of the remaining cells in G0/G1, S, and G2/M phases was expressed as DNA histogram by using MultiCycle software.

In vitro migration assay

HUVECs were seeded and then starved with medium containing 0.5% FBS for 6 h. After wounded by pipette tips, cell were incubated in fresh medium with and without 50 ng/mL VEGF and various concentrations of Ru complexes. After incubated for indicated times, migrated cells were photographed and quantified by manual counting in three independent experiments.

Invasion assay

Effects of Ru complexes on the invasion of HUVECs were performed on Transwell Boyden chamber (8 μm pore, Corning, Lowel, MA) pre-coated with matrigel for 4 h at 37°C. The upper compartment of chamber supplemented with 0.1% FBS medium containing 100 μL of suspending HUVECs cell (5×10^4 cells), while the bottom chambers were added with 500 μL ECGM with 10% FBS and mixed with desired concentrations of Ru complexes and 50 ng/mL VEGF. After incubated for 24 h, the non-migrant cells from the upper face of the Transwell membrane were removed and invaded cells were fixed and stained with Giemsa solution. Images of migrant cells were quantified by manual counting in three independent experiments.

Tube formation assay

Matrigel was thawed at 4°C and each well of prechilled 48-well plates was coated with 100 μL Matrigel and incubated at 37°C for 45 min. HUVECs (4–5×10^4) with desired concentration of Ru complexes and 50 ng/mL VEGF were added to the matrigel layer. After 8-10 h, the tube formation was visualized under an

inverted microscope. Three independent experiments were performed.

Matrigel plug assay

Five 6-weeks old male C57/BL/6 mice were injected with Matrigel (0.5 mL/plug) containing VEGF (50 ng/mL) and different concentrations of Ru complex in each group. The plugs were removed after 7 d incubation, fixed and embedded for H&E staining. Drabkin method was involved to measure hemoglobin content, which as indication of blood vessel formation.

Chorioallantoic membrane assay

The anti-angiogenesis effect of Ru(II) complexes on the *ex ovo* was determined by CAM assay. Briefly, fertilized chicken eggs were incubated at 37°C in a humidified incubator. On embryonic day-7 or -8, eggs were cracked open and methylcellulose discs containing different concentrations of Ru(II) complex (20 or 40 μg /egg) and VEGF (50 ng/mL) were gently implanted on top of chicken CAM then the embryos were incubated for another 2 days. Two days later, the CAM was observed under a microscope (Olympus BX 40) and photographed. VEGF was used as a positive control. Six eggs per group were used in each experiment and three independent experiments were performed. The vascular density of CAM images were quantified with the use of Image Pro-Plus software.

Measurement of ROS generation and antioxidant activity

The intracellular ROS generation in HUVECs exposed to different Ru complexes for different periods of time was detected by DCFH-DA.[43] The free radical scavenging activities of the synthetic Ru complexes were examined by ABTS and DPPH free radical scavenging assays as previously described[42].

Western blot analysis

The effects of the synthetic Ru complexes on expression levels of the proteins related with the anti-angiogenic effects were determined by Western blot analysis.[44]

Statistical analysis

Experiments were repeated at least for three times. Statistical analysis was performed using SPSS statistical package (SPSS 13.0 for Windows; SPSS, Inc. Chicago, IL).

Notes and references

Department of Chemistry, Jinan University, Guangzhou 510632, China.

E-mail: tchentf@jnu.edu.cn; Fax:+86 20 85221263; Tel:+86 20-85225962

* E-mail: tchentf@jnu.edu.cn.

‡Authors contributed equally to the work.

† Electronic Supplementary Information (ESI) available: ESI-MS and ^{1}H NMR of complex **2** and **3**, UV-Vis spectra of Ru complexes in PBS buffer. See DOI: 10.1039/c000000x/

1 Weis, S. M.; Cheresh, D. A. *Nat. Med.* **2011**, *17*, 1359-1370.
2 Carmeliet, P.; Jain, R. K. *Nature* **2011**, *473*, 298-307.
3 Kowanetz, M.; Ferrara, N. *Clin. Cancer Res.* **2006**, *12*, 5018-5022.
4 Chi, A. S.; Norden, A. D.; Wen, P. Y. *Neurotherapeutics* **2009**, *6*, 513-526.
5 Weis, S. M.; Cheresh, D. A. *Nature* **2005**, *437*, 497-504.
6 Sherwood, L. M.; Parris, E. E.; Folkman, J. *N. Engl. J. Med.* **1971**, *285*, 1182-1186.
7 Tugues, S.; Koch, S.; Gualandi, L.; Li, X.; Claesson-Welsh, L. *Mol. Aspects Med.* **2011**, *32*, 88-111.
8 Cho, S. G.; Yi, Z.; Pang, X.; Yi, T.; Wang, Y.; Luo, J.; Wu, Z.; Li, D.; Liu, M. *Cancer Res.* **2009**, *69*, 7062-7070.
9 Xin, H.; Herrmann, A.; Reckamp, K.; Zhang, W.; Pal, S.; Hedvat, M.; Zhang, C.; Liang, W.; Scuto, A.; Weng, S. *Cancer Res.* **2011**, *71*, 6601-6610.
10 Meyer, A.; Bagowski, C. P.; Kokoschka, M.; Stefanopoulou, M.; Alborzinia, H.; Can, S.; Vlecken, D. H.; Sheldrick, W. S.; Wolfl, S.; Ott, I. *Angew. Chem. Int. Edit.* **2012**, *51*, 8895-8899.
11 Bagowski, C. P.; You, Y.; Scheffler, H.; Vlecken, D. H.; Schmitza, D. J.; Ott, I. *Dalton Trans.* **2009**, 10799-10805.
12 Ott, I.; Qian, X. H.; Xu, Y. F.; Vlecken, D. H. W.; Marques, I. J.; Kubutat, D.; Will, J.; Sheldrick, W. S.; Jesse, P.; Prokop, A.; Bagowski, C. P. *J. Med. Chem.* **2009**, *52*, 763-770.
13 Ott, I.; Kircher, B.; Bagowski, C. P.; Vlecken, D. H. W.; Ott, E. B.; Will, J.; Bensdorf, K.; Sheldrick, W. S.; Gust, R. *Angew. Chem. Int. Edit.* **2009**, *48*, 1160-1163.
14 Nowak-Sliwinska, P.; van Beijnum, J. R.; Casini, A.; Nazarov, A. A.; Wagnieres, G.; van den Bergh, H.; Dyson, P. J.; Griffioen, A. W. *J. Med. Chem.* **2011**, *54*, 3895-3902.
15 Zou, T. T.; Lum, C. T.; Lok, C. N.; To, W. P.; Low, K. H.; Che, C. M. *Angew. Chem. Int. Edit.* **2014**, *53*, 5810-5814.
16 Streu, C.; Feng, L.; Carroll, P. J.; Maksimoska, J.; Marmorstein, R.; Meggers, E. *Inorg. Chim. Acta* **2011**, *377*, 34-41.
17 Chen, T.; Liu, Y.; Zheng, W.-J.; Liu, J.; Wong, Y.-S. *Inorg. Chem.* **2010**, *49*, 6366-6368.
18 Li, L.; Cao, W.; Zheng, W.; Fan, C.; Chen, T. *Dalton Trans.* **2012**, *41*, 12766-12772.
19 Liu, M. M.; Lim, Z. J.; Gwee, Y. Y.; Levina, A.; Lay, P. A. *Angew. Chem. Int. Edit.* **2010**, *49*, 1661-1664.
20 Nowak-Sliwinska, P.; van Beijnum, J. R.; Casini, A.; Nazarov, A. A.; Wagnières, G.; van den Bergh, H.; Dyson, P. J.; Griffioen, A. W. *J. Med. Chem.* **2011**, *54*, 3895-3902.
21 Sava, G.; Zorzet, S.; Turrin, C.; Vita, F.; Soranzo, M.; Zabucchi, G.; Cocchietto, M.; Bergamo, A.; DiGiovine, S.; Pezzoni, G. *Clin. Cancer. Res.* **2003**, *9*, 1898-1905.
22 Scolaro, C.; Bergamo, A.; Brescacin, L.; Delfino, R.; Cocchietto, M.; Laurenczy, G.; Geldbach, T. J.; Sava, G.; Dyson, P. J. *J. Med. Chem.* **2005**, *48*, 4161-4171.
23 Clavel, C. M.; Paunescu, E.; Nowak-Sliwinska, P.; Griffioen, A. W.; Scopelliti, R.; Dyson, P. J. *J. Med. Chem.* **2014**, *57*, 3546-3558.
24 Yang, L. C.; Zhang, J. N.; Wang, C.; Qin, X. Y.; Yu, Q. Q.; Zhou, Y. H.; Liu, J. *Metallomics* **2014**, *6*, 518-531.
25 Li, L.; Wong, Y. S.; Chen, T.; Fan, C.; Zheng, W. *Dalton Trans.* **2012**, *41*, 1138-1141.
26 Boiani, M.; Gonzalez, M. *Mini-Rev. Med. Chem.* **2005**, *5*, 409-424.
27 Bhaumik, C.; Das, S.; Saha, D.; Dutta, S.; Baitalik, S. *Inorg. Chem.* **2010**, *49*, 5049-5062.
28 Bhaumik, C.; Saha, D.; Das, S.; Baitalik, S. *Inorg. Chem.* **2011**, *50*, 12586-12600.
29 Boča, M.; Jameson, R. F.; Linert, W. *Coord. Chem. Rev.* **2011**, *255*, 290-317.

30 Maity, D.; Das, S.; Mardanya, S.; Baitalik, S. *Inorg. Chem.* **2013**, *52*, 6820-6838.

31 Yellol, G. S.; Donaire, A.; Yellol, J. G.; Vasylyeva, V.; Janiak, C.; Ruiz, J. *Chem. Commun.* **2013**, *49*, 11533-11535.

32 Yellol, G. S.; Yellol, J. G.; Kenche, V. B.; Liu, X. M.; Barnham, K. J.; Donaire, A.; Janiak, C.; Ruiz, J. *Inorg. Chem.* **2014**, DOI: 10.1021/ic502119b.

33 Sun, H. L.; Tsai, A. C.; Pan, S. L.; Ding, Q. Q.; Yamaguchi, H.; Lin, C. N.; Hung, M. C.; Teng, C. M. *Clin. Cancer Res.* **2009**, *15*, 4904-4914.

34 Kerbel, R. S. *N. Engl. J. Med.* **2008**, *358*, 2039-2049.

35 Xiao, D.; Singh, S. V. *Cancer Res.* **2007**, *67*, 2239-2246.

36 Pang, X.; Yi, T.; Yi, Z.; Cho, S. G.; Qu, W.; Pinkaew, D.; Fujise, K.; Liu, M. *Cancer Res.* **2009**, *69*, 518-525.

37 Ushio-Fukai, M.; Nakamura, Y. *Cancer Lett.* **2008**, *266*, 37-52.

38 Wu, Q.; Fan, C.; Chen, T.; Liu, C.; Mei, W.; Chen, S.; Wang, B.; Chen, Y.; Zheng, W. *Eur. J. Med. Chem.* **2013**, *63*, 57-63.

39 Zhao, Z.; Luo, Z.; Wu, Q.; Zheng, W.; Feng, Y.; Chen, T. *Dalton Trans.* **2014**, *43*, 17017-17028.

40 Pierroz, V.; Joshi, T.; Leonidova, A.; Mari, C.; Schur, J.; Ott, I.; Spiccia, L.; Ferrari, S.; Gasser, G. *J. Am. Chem. Soc.* **2012**, *134*, 20376-20387.

41 Zhang, Y.; Li, X.; Huang, Z.; Zheng, W.; Fan, C.; Chen, T. *Nanomed. Nanotechnol. Biol. Med.* **2013**, *9*, 74-84.

42 Chen, T.; Wong, Y.-S.; Zheng, W.; Liu, J. *Chem. Biol. Interact.* **2009**, *180*, 54-60.

43 Luo, Z. D.; Yu, L. L.; Yang, F.; Zhao, Z. N.; Yu, B.; Lai, H. Q.; Wong, K. H.; Ngai, S. M.; Zheng, W. J.; Chen, T. F. *Metallomics* **2014**, *6*, 1480-1490.

44 Fan, C.; Chen, J.; Wang, Y.; Wong, Y.-S.; Zhang, Y.; Zheng, W.; Cao, W.; Chen, T. *Free Radical Biol. Med.* **2013**, *65*, 305-316.

Metallomics Accepted Manuscript